New Slip Regimes and the Shape of Dewetting Thin Liquid Films

R. Fetzer and K. Jacobs
Department of Experimental Physics, Saarland University, 66041 Saarbrücken, Germany

A. Münch
Institute of Mathematics, Humboldt University Berlin, 10099 Berlin, Germany and WIAS, Mohrenstraße 39, 10117 Berlin, Germany

B. Wagner
WIAS, Mohrenstraße 39, 10117 Berlin, Germany

T. P. Witelski
Department of Mathematics, Duke University, Durham, North Carolina 27708-0320, USA
(Received 20 December 2004; published 14 September 2005)

We compare the flow behavior of liquid polymer films on silicon wafers coated with either octadecyl- (OTS) or dodecyltrichlorosilane (DTS). Our experiments show that dewetting on DTS is significantly faster than on OTS. We argue that this is tied to the difference in the solid/liquid friction. As the film dewets, the profile of the rim advancing into the undisturbed film is monotonically decaying on DTS but has an oscillatory structure on OTS. For the first time we can describe this transition in terms of a lubrication model with a Navier-slip condition for the flow of a viscous Newtonian liquid.

DOI: 10.1103/PhysRevLett.95.127801 PACS numbers: 68.15.+e, 47.20.Ma, 47.54.+r, 68.37.Ps

Thin films of liquid polymers play an important role in numerous technological processes ranging from lithography to biological membranes [1]. In recent years, one major focus of interest has been to understand the dynamics and morphology of polymer films dewetting from hydrophobic substrates. The film thickness typically ranges on the scale of tens to a few hundred nanometers. Dewetting starts with the formation of holes due to spinodal dewetting or heterogeneous nucleation. As the holes grow, the displaced liquid collects in growing rims surrounding the holes.

Many studies have focused on this dynamics following rupture [1–11], e.g., on the appearance of a rim, or on the presence or vanishing of a damped oscillatory structure that joins the rim to the external undisturbed film. Concerning the latter problem the authors of Refs. [2–4] proposed to include viscoelastic effects into their model in order to explain the profiles of the monotonically decaying rims that were experimentally observed for longer chained polymer films [5]. In Ref. [11] shear-thinning properties of the polymer film were included to explain such differing morphologies. With these arguments, however, one has omitted the fact that slippage at the solid/liquid interface, the magnitude of which is altered by changing the molecular weight [6], may also have an effect on the dewetting dynamics.

In this Letter we present a study of how the morphology of the dewetting rim can be affected by slippage. The occurrence and the nature of slippage of liquids on solid surfaces is extensively discussed in the literature [6–10], and is of large technological interest since a sliding fluid can flow faster, e.g., through microfluidic devices.

We describe experiments where, for the first time, we are able to change the boundary condition at the substrate independently from viscoelastic properties of the liquid. We investigate the dewetting dynamics and morphology of thin films of atactic polystyrene of low molecular weight on oxidized Si wafers. To change the boundary condition at the solid/liquid interface without influencing the contact angle of the melt, the wafers are coated with either a monolayer of octadecyltrichlorosilane (OTS) or with dodecyltrichlorosilane (DTS), while keeping all other properties of the substrate and the liquid fixed. Hence, we can directly study the influence of slippage on the dewetting dynamics.

Our experiments show that if OTS is used the shape of the rim develops a damped oscillatory structure towards the undisturbed film, while for a DTS coating the rim decays monotonically. A potential explanation for this surprising behavior is provided by a comparison of the dewetting rates, which are markedly higher for DTS, indicating a lower friction coefficient, and hence higher slippage, for this type of coating.

We develop a mathematical model that is able to predict these experimental findings on the basis of purely viscous and slippage effects. This model can be derived from the Navier-Stokes equations together with the Navier-slip boundary condition. Making use of the scale separation between the height of the film H and the lateral dimension of the rim L, we find two distinguished limits that lead to two different lubrication models, depending on the order of magnitude of the slip length. The slip length can be understood as the length below the solid/liquid interface where the velocity extrapolates to zero [8,9]. For a slip length that

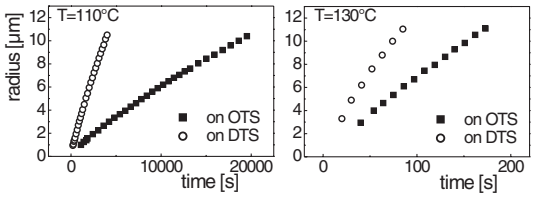

FIG. 1. The growth of hole radii of dewetted regions as a function of time on OTS/DTS substrates at three different temperatures.

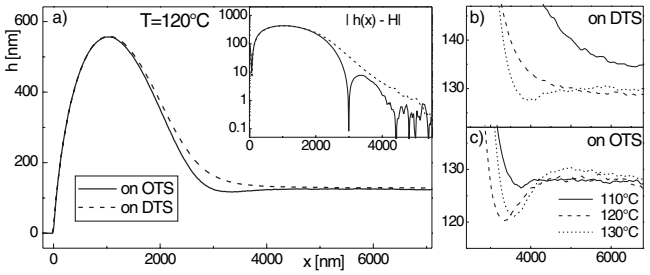

FIG. 2. Rim profiles of 130 nm PS films on DTS and OTS covered Si wafers (a) at constant temperature (the inset depicts a semilog plot of $|h(x) - H|$), (b) and (c) at three different temperatures on DTS and OTS surfaces, respectively. Profiles are shown with the three-phase contact line shifted into the origin.

is small, or at most of the order of the thickness of the dewetting film, we obtain the well-known lubrication equation [1]. When the slip length is assumed to be much larger than the thickness of the film, we obtain a different lubrication model consisting of a system of equations for the profile and the velocity of the film. We show that this second model captures the disappearance of the capillary waves behind the rim for sufficiently large slip length, which compares well with our experimental results. This suggests that for many microfluidic flows, slip effects may dominate the dynamics and control morphological instabilities that occur in dewetting.

The liquid used in our experiments was atactic polystyrene (PS) with a molecular weight of 13.7 kg/mol ($M_w/M_n = 1.03$). The samples were prepared by spin casting a toluene solution of PS onto mica, floating the films on Millipore^{TM} water, and then picking them up with our wafers. We used two different silane coatings of the Si wafer (2.1 nm native oxide layer), OTS and the shorter DTS, respectively, prepared by standard techniques [12]. The thicknesses of these self-assembled monolayers measured by ellipsometry are $d_{\mathrm{OTS}} = 2.3(3)$ nm and $d_{\mathrm{DTS}} = 1.5(2)$ nm. Surface characterization by scanning probe microscopy (SPM) revealed a RMS roughness of 0.09(1) nm (OTS) and 0.13(2) nm (DTS), and an equilibrium contact angle of polystyrene droplets of 68(2)° and 66(2)°, respectively.

All PS films in this study are 130(5) nm thick. To induce dewetting, the films were heated to three different temperatures (110 °C, 120 °C, 130 °C). After a few seconds circular holes appear due to heterogeneous nucleation and grow rapidly [13]. The radii of the emerging holes in the PS(13.7 k) film were measured by optical microscopy. As shown in Fig. 1, dewetting progresses more quickly on DTS than on OTS coated substrates.

After quenching the samples (with holes of identical diameter of 22(1) μm) to room temperature, we measured the glassy rim profiles [14] by SPM (Multimode, Digital Instruments, Santa Barbara, USA) in Tapping Mode^{TM}. Figure 2 demonstrates that the type of substrate affects the rim profile: On OTS covered substrates, the rim of the dewetting PS film exhibits an oscillatory shape, whereas on DTS covered surfaces, at the same temperature, no oscillation is observed. The inset to Fig. 2(a) clarifies the oscillatory rim shape on OTS by plotting $|h(x) - H|$ in a semilog plot for 120 °C where H denotes the initial thickness of the film. To account for the influence of viscosity, we compare the results on DTS and on OTS for three different dewetting temperatures, cf., Figs. 2(b) and 2(c), respectively. On DTS we are able to induce an oscillatory shape for 130 °C.

We explain these results as follows. At the same temperature the liquids on both samples have exactly the same properties: the viscosity μ as well as the surface tension σ do not depend on the substrate underneath. Additionally, the contact angle of polystyrene on both surfaces is constant within the experimental error. Therefore, the spreading coefficient $S = \sigma(1 - \cos\theta)$, that is the driving force of the dewetting process, is identical for OTS and DTS. The only change can be the short-range interaction at the solid/liquid interface.

Indeed the contact angles of apolar liquids like bicyclohexyl vary on both coatings. We find $43(1)^{\circ}$ on OTS and $36(2)^{\circ}$ on DTS. Via the Good-Girifalco equation, the contact angle of apolar liquids is directly linked to the surface energy of the substrate [15]. Thus, we find a larger surface energy σ_s for DTS than for OTS covered Si wafers. Using Young's equation $\sigma\cos\theta = \sigma_s - \sigma_{sl}$, identical contact angle of PS on both substrates yields to different energies σ_{sl} at the OTS/PS and DTS/PS interface, respectively. Note that polystyrene has polar contributions. Therefore, surface energies cannot be determined directly from contact angle measurements of PS only.

The larger interface energy of the DTS coating might be a possible explanation for the significantly larger dewetting velocity of PS(13.7 k) we observe on DTS compared to OTS at same driving force. One may think, e.g., of a coil-stretch transition of the polymer chains in the vicinity of the substrate that depend on the interface energy [16]. This conformational change results in an enhanced velocity, described by slippage.

Another molecular explanation for the different slip lengths might be that the PS chains interdiffuse differently into the two types of brushes, OTS and DTS.

We introduce a theoretical model describing this dewetting scenario by taking into account large variations of slip.

We start with the 2D Navier-Stokes equations for viscous incompressible Newtonian flow [17], $\rho(\partial_t \mathbf{u} + \mathbf{u}\cdot\nabla\mathbf{u}) = -\nabla[p + \phi(h)] + \mu\nabla^2\mathbf{u}$ and $\nabla\cdot\mathbf{u} = 0$, with $\mathbf{u} = (u, w)$ the velocity, ρ the density, μ the viscosity of the liquid, p the pressure, and $\phi(h)$ the disjoining pressure of the two systems. The disjoining pressure consists of a Born repulsion term and a van der Waals part with destabilizing term that drives the dewetting [18–20]. We assume that for holes whose radii are large compared to the width of the rim, the influence of the rim curvature is weak and can be neglected. For the 2D free surface flow we have the usual normal and tangential stress conditions at the free surface and the kinematic condition $\partial_t h = w - u\partial_x h$ for the film thickness $z = h(x, t)$. On the solid surface we have impermeability $w = 0$ and a Navier-slip condition $u = b\partial_z u$, where b is the slip length. We nondimensionalize $(z^*, h^*, b^*) = (z, h, b)/H$ and $x^* = x/L$, where L is the typical lateral scale of the dewetting rim, with $\varepsilon = H/L \ll 1$. Similarly $(u^*, \varepsilon w^*) = (u, w)/U$, $(p^*, \phi^*) = (p, \phi)/P$, $t^* = \varepsilon U/Ht$, where $P = \mu U/(\varepsilon H)$, $U = \sigma\varepsilon^3/\mu$ with σ being the constant surface tension. If the dimensionless slip length $b \sim O(1)$, we obtain, to leading order in ε, the lubrication equation $\partial_t h = -\partial_x\{(h^3/3 + bh^2)\partial_x[\partial_x^2 h - \phi'(h)]\}$ for weak slippage, where we have dropped the stars. However, for this model, the rims always have a spatially oscillatory shape as is known from previous investigations [2].

If, however, the slip length is large, we rescale the velocity as $u = b\tilde{u}$ and time as $t = \tilde{t}/b$, i.e., in effect scaling the velocity scale U with b. We then find a regime of $b = \beta/\varepsilon^2$, which yields a different lubrication model (dropping the tildes)

$$\partial_t h + \partial_x(hu) = 0, \tag{1}$$

$$\beta\,\mathrm{Re}(\partial_t u + u\partial_x u) = \frac{4\beta}{h}\partial_x(h\partial_x u) + \partial_x[\partial_x^2 h - \phi'(h)] - \frac{u}{h}, \tag{2}$$

with the Reynolds number $\mathrm{Re} = \rho\sigma H/\mu^2$. The two models we have introduced so far are embedded in a whole family of lubrication models that can be derived for different regimes of the slip length. The other regimes are the no-slip regime, the intermediate regime, and the lubrication model describing retracting free films. The intermediate regime is obtained for slip lengths of order $b = \beta/\varepsilon^\alpha$ with $0 < \alpha < 2$. It also arises from (1) and (2) in the limit $\beta \to 0$, which yields a scalar lubrication equation with an h^2 mobility. Some recent results on the contact-line instability of dewetting thin films in this regime can be found in Ref. [21]. The model for retracting free films, see [22], is recovered by rescaling u with β and then letting $\beta \to \infty$. This regime corresponds to $b \gg \beta/\varepsilon^2$. A more detailed derivation of all these regimes from the Navier-Stokes equations, asymptotic analysis, and comparison to numerical results can be found in Ref. [23]. A similar derivation of the lubrication models has just appeared in Ref. [24].

We seek an approximate description of the portion of the profile of the dewetting rim that connects to the undisturbed uniform film $h = 1$ for $x \to \infty$. Consistency with Eqs. (1) and (2) requires that $u \to 0$ as $x \to \infty$. It is convenient to shift to a comoving frame of reference $\xi = x - s(t)$, where $s(t)$ denotes the position of the contact line. Near the flat state, the evolution can be described by introducing the ansatz $h(x, t) = 1 + \delta\varphi(\xi)$, $u = \delta v(\xi)$, $\delta \ll 1$, into Eqs. (1) and (2). Keeping only the $O(\delta)$ terms yields

$$-\dot{s}^2\beta\,\mathrm{Re}\,\partial_\xi\varphi = 4\dot{s}\beta\partial_\xi^2\varphi + \partial_\xi^3\varphi - \dot{s}\varphi. \tag{3}$$

We have to note here that we neglect the effect of the slowly growing rim. We consider the normal mode solutions $\varphi(\xi) = e^{\omega\xi}$ of (3) which decay for $\xi \to \infty$. If the discriminant

$$D = \frac{4\dot{s}^4\beta^3}{3^3}(\mathrm{Re} - 4\beta)\mathrm{Re}^2 + \frac{8\beta^2\dot{s}^2}{3}\mathrm{Re} - \frac{4^4\beta^3\dot{s}^2}{3^3} + 1 \tag{4}$$

is positive, then φ has spatial oscillations due to a pair of complex conjugate ω. Hence, the rim is a damped capillary wave. But if D is negative the complex conjugate ω is replaced by two real modes, which allow the solution $\varphi(\xi)$ to decay monotonically for $\xi \to \infty$. In our case, Re is extremely small and can be neglected, so that the transition from complex conjugate to real decaying modes occurs when $\beta > \beta_{\mathrm{th}}(\dot{s}) = (3/4)/(4\dot{s}^2)^{1/3}$. Equivalently, this can be written as $b_{\mathrm{th}} = (3/4)^3/(4\dot{s}_{\mathrm{fig}}^2)$, where $\dot{s}_{\mathrm{fig}} = \varepsilon^3\dot{s}^*$ is the contact-line velocity nondimensionalized with σ/μ. This threshold is shown in Fig. 3. The transition from complex conjugate to real decaying modes can also be found from the full Stokes equation. In Fig. 3 we also show the corresponding threshold that was numerically obtained from the normal mode solution of the linearized Stokes problem. The figure shows that they compare well except for small slip lengths.

The diagram in Fig. 3 allows predictions regarding the shape of the dewetting rim only if both the dimensionless slip length b and speed $\dot{s}_{\mathrm{fig}}$ of the wave are known. The contact-line speed depends on the slip length and can be obtained from simulations of dewetting fronts using Eqs. (1) and (2). The dashed line shows the value for the

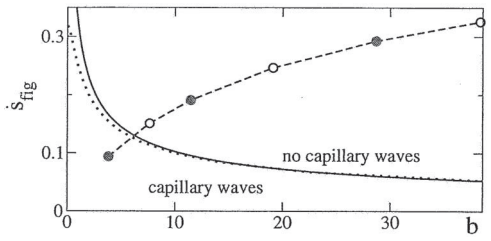

FIG. 3. Transition curves in $(b, \dot{s}_{\mathrm{fig}})$ parameter space for profiles with and without capillary waves, calculated from the lubrication model (solid line) and Stokes model (dotted line). The dashed line shows the contact-line speed for different slip lengths, calculated from the lubrication model.

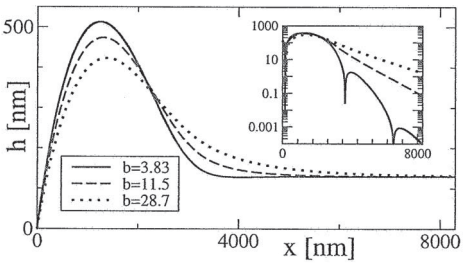

FIG. 4. Rim profiles for different slip lengths b nondimensionalized with $H = 130$ nm. The inset shows a semilog plot of $|h(x) - H|$.

dewetting rate when the cross sections of the rims have the same area as those found in our experiments. The values of the slip length that were used in the simulations for the three profiles shown Fig. 4 are the same as for the filled circles in Fig. 3.

One observes that as b is increased, the dewetting rate increases and for slip lengths larger than about six, the dashed line in Fig. 3 leaves the region where capillary waves are expected. Indeed, the profiles in the simulations show a dip for the smallest $b = 3.83$, but monotone profiles for $b > 6$. Closer inspection of the profile in a semilog plot shows a second maximum for the smallest b, indicating that we have the oscillatory structure of a wave, which however decays very rapidly for increasing x.

We finally note that, since the contact angles here are not small, it is reasonable to compare our results using the linearized curvature in Eq. (2) with those, where the fully nonlinear curvature is accounted for, in a similar fashion as done, e.g., in [25]. We found from our simulations that in this case only the dewetting rates for large b are affected in that they are modestly decreased; the profiles, however, remain very close to those presented above.

Comparing now the theoretical results with the experimental observations, we find them in good qualitative agreement: At $T = 120\,^{\circ}\mathrm{C}$, a dip is only seen in the rim on the OTS coated wafer, where slippage is smaller according to the dewetting rates than for the DTS coated wafer. Repeating the experiment at lower and higher temperature confirms this trend that the oscillations are suppressed, i.e., smaller or even absent, on the DTS wafer. The linearized analysis and the numerical computations for the film profiles show the same behavior: Increasing the slip length for otherwise fixed parameters suppresses the spatially oscillatory structure on the side of the rim facing the undisturbed film.

To conclude, we have shown that the transition from an oscillating to a monotonically decaying dewetting rim profile that has been observed for the first time by solely changing the friction at the substrate can be captured by a lubrication model for Newtonian liquids in a regime of large slip lengths.

A. M. acknowledges support via DFG Grant No. MU 1626/3 and by the DFG research center MATHEON, Berlin. R. F. and K. J. acknowledge support by Grant No. JA 905/3 within the DFG priority program 1164, and generous support by Siltronic AG, Burghausen, Germany. T. W. is grateful for the hospitality of WIAS and HU and was supported by NSF Grant Nos. 0244498 and 0239125.

[1] A. Oron, S. H. Davis, and S. G. Bankoff, Rev. Mod. Phys. **69**, 931 (1997).
[2] R. Seemann, S. Herminghaus, and K. Jacobs, Phys. Rev. Lett. **87**, 196101 (2001).
[3] S. A. Safran and J. Klein, J. Phys. II (France) **3**, 749 (1993).
[4] S. Herminghaus, R. Seemann, and K. Jacobs, Phys. Rev. Lett. **89**, 056101 (2002).
[5] G. Reiter, Phys. Rev. Lett. **87**, 186101 (2001).
[6] P. de Gennes, Rev. Mod. Phys. **57**, 827 (1985).
[7] L. Bureau and Léger, Langmuir **20**, 4523 (2004), and references therein.
[8] F. Brochard-Wyart, C. Gay, and P. de Gennes, Macromolecules **29**, 377 (1996).
[9] L. Léger, J. Phys. Condens. Matter **15**, S19 (2003).
[10] E. Lauga, M. P. Brenner, and H. A. Stone, cond-mat/0501557vI [*Handbook of Experimental Fluid Dynamics* (to be published)].
[11] F. Saulnier, E. Raphaël, and P. G. de Gennes, Phys. Rev. E **66**, 061607 (2002).
[12] S. Wasserman, S. R. Y.-T. Tao, and G. M. Whitesides, Langmuir **5**, 1074 (1989).
[13] K. Jacobs, S. Herminghaus, and K. R. Mecke, Langmuir **14**, 965 (1998).
[14] Comparing glassy with liquid profiles we could not detect any difference in shape.
[15] R. J. Good and L. A. Girifalco, J. Phys. Chem. **64**, 561 (1960).
[16] F. Brochard and P. de Gennes, Langmuir **8**, 3033 (1992).
[17] Though we cannot strictly exclude viscoelastic effects, we neglect them here, since the chain length of PS (l3.7 k) is below the entanglement length of PS, and our experiments were done at extremely low shear rates.
[18] S. Dietrich, in *Phase Transitions and Critical Phenomena*, edited by C. Domb and J. Lebowitz (Academic, New York, 1988).
[19] M. Schick, in *Liquids and Interfaces*, edited by J. C. *et al.* (Elsevier, New York, 1989).
[20] R. Seemann, S. Herminghaus, and K. Jacobs, Phys. Rev. Lett. **86**, 5534 (2001).
[21] A. Münch and B. Wagner, Physica D (Amsterdam) **209**, 178 (2005).
[22] T. Erneux and S. H. Davis, Phys. Fluids A **5**, 1117 (1993).
[23] A. Münch, B. Wagner, and T. Witelski (to be published).
[24] K. Kargupta, A. Sharma, and R. Khanna, Langmuir **20**, 244 (2004).
[25] A. Münch, J. Phys. Condens. Matter **17**, 309 (2005).